第 31 卷第 9 期
2015 年 9 月

无 机 化 学 学 报
CHINESE JOURNAL OF INORGANIC CHEMISTRY

Vol.31 No.9
1903-1912

金纳米粒表面修饰官能团及其影响细胞作用的机制

文长春 雷文琪 沈星灿* 纪仕辰 蒋邦平 梁 宏*
(广西师范大学药用资源化学与药物分子工程教育部重点实验室,桂林 541004)

摘要: 通过配体交换法,在 AuNPs 表面分别引入羟基(-OH),羧基(-COOH)和甲基(-CH_3),制备了 3 种表面修饰官能团的金纳米粒:Au-OH NPs,Au-COOH NPs 和 Au-CH_3 NPs,其平均粒径为(15.6±3.2) nm,ζ 电位均为负值。MTT 法对比研究表面修饰和未修饰的 AuNPs 与 HeLa 细胞和 MCG-803 细胞作用后的细胞存活率,当浓度达到 197 ng·mL^{-1} 时,表现出低细胞毒性,且顺序为:AuNPs>Au-CH_3 NPs>Au-COOH NPs≈Au-OH NPs。细胞周期研究结果发现,表面未修饰的 AuNPs 对细胞 G2/M 期活动有一定的阻滞作用。单个活细胞显微拉曼光谱原位对比研究表面修饰和未修饰的 AuNPs 与 HeLa 细胞的作用,结果表明:未修饰的 AuNPs 和 Au-CH_3 NPs 与细胞作用的主靶点可能为 DNA 骨架、碱基和细胞磷脂膜的极性头部,而 Au-COOH NPs 与 Au-OH NPs 对这些位点作用轻微。本研究为解释表面修饰-COOH 和-OH 官能团可降低 AuNPs 细胞毒性提供了研究证据。

关键词: 金纳米粒; 表面官能团; 细胞毒性; 分子机制
中图分类号: O614.123 **文献标识码**: A **文章编号**: 100-4861(2015)09-1903-10
DOI: 10.11862/CJIC.2015.253

Comparative Interaction Mechanisms Between Cells and Gold Nanoparticles Modified with Different Chemical Functional Groups

WEN Chang-Chun LEI Wen-Qi SHEN Xing-Can* JI Shi-Chen JIANG Bang-Ping LIANG Hong*
(*Key Laboratory of Medicinal Chemical Resources and Molecular Engineering, Ministry of Education, Guangxi Normal University, Guilin* 541004, *China*)

Abstract: Chemical functional groups of -CH_3, -COOH and -OH have been introduced to the surface of AuNPs, separately. The AuNPs, Au-OH NPs, Au-COOH NPs and Au-CH_3 NPs are spherical with dimension of (15.6±3.2) nm, displaying negative ζ potentials. The cytotoxicity of these AuNPs has been evaluated by methylthiazoletetrazolium (MTT) assay against Hela cells and MCG-803 cells *in vitro*, separately. MTT data reveal that the surface unmodified AuNPs exhibit low cytotoxicity at the highest concentration of 197 ng·mL^{-1} for both HeLa and MCG-803 cells in vitro. The surface modified AuNPs can further decrease the inherently cytotoxicity that follows the order AuNPs>Au-CH_3 NPs>Au-COOH NPs≈Au-OH NPs. Cell cycle analysis indicates that AuNPs cause cell cycle slightly arrest at the G_2/M phase. Micro-Raman spectra of individual living HeLa cells demonstrate that the backbone and nucleic bases of DNA as well as the polar headgroup of phospholipid in cells are the probable target binding sites of AuNPs and Au-CH_3 NPs. Whereas, the interfacial interactions are significantly reduced when cells are treated with Au-COOH NPs and Au-OH NPs. Our results on the interaction mechanisms between AuNPs and cells demonstrate that AuNPs modified with surface functional groups of -COOH or -OH can improve their cytocompatibility.

Key words: gold nanoparticles (AuNPs); surface functional groups; cycotoxicity; molecular mechanisms

收稿日期:2015-06-18。收修改稿日期:2015-08-04。
国家自然科学基金(No.21161003, 21364002),广西自然科学基金杰青(2013GXNSFGA019001),教育部新世纪优秀人才支持计划(NCET-13-0743),药用资源化学与药物分子工程教育部重点实验室主任基金(2015-A)资助项目。
*通讯联系人。E-mail:xcshen@mailbox.gxnu.edu.cn; hliang@gxnu.edu.cn, Tel: +86-0773-5846273;会员登记号:05M140629103。

0 Introduction

Over the past decades, gold nanoparticles (AuNPs) have attracted enormous amount of interest for biomedical applications based on their unique optical, chemical, electrical, and catalytic of properties[1-2]. The classic ways to prepare AuNPs are chemical reduction of gold chloride with citrate-mediated reductions in boiling water[3], or with sodium borohydride in the presence of alkane thiols in a water-toluene phase[4]. The reliable AuNPs have been synthesized, and surface coatings provide their both solubility and stability[1-6]. The strong binding of thiols, phosphines and amines to AuNPs enables easy surface functionalization of AuNPs with various materials, such as polymers[6-7], silica[8], enzymes[9], peptide[10], protein[11], miRNA[12], drugs[13-14] and targeting agents[8,14], leading to important biomedical applications including X-ray/CT imaging, cell imaging, targeted drug delivery, cancer diagnostics and therapeutic agents[6-14]. The new and exciting advances on AuNPs in biology and medicine have been reviewed[1,5,15-16].

For most of the fascinated cellular and therapeutic uses, AuNPs are often required to pass cell plasma membranes either by endocytosis or by direct penetration to reach target cellular compartments[17]. Thus, the interaction of AuNPs with biological systems has become one of the most urgent areas for their bio-applications and toxicological studies. Numerous experimental studies have been conducted to probe AuNPs-cell interactions in the past few years. It has been reported that the size and surface charges can dramatically influence the uptake of AuNPs, showing that cationic 2-nm AuNPs are moderately toxic, whereas anionic 2-nm AuNPs are quite nontoxic[18], and revealing that both the level of penetration and membrane disruption increase as surface charge density of the AuNPs increases[7]. In addition, surface modifications can also lead to different AuNPs-cell interactions[6-21]. The 18-nm spherical AuNPs with citrate and biotin are not inherently toxic at concentrations up to 250 $\mu mol \cdot L^{-1}$ (gold atoms), whereas, those capped with glucose or cysteine surface modifiers, or with a reduced gold surface, were nontoxic at concentrations up to 25 $\mu mol \cdot L^{-1}$ (gold atoms)[19]. It was reported that 1.4-nm AuNPs stabilized by triphenylphosphine derivatives causes predominantly rapid cell death via necrosis by oxidative stress, whereas, AuNPs of similar size but capped with glutathione likewise do not induce oxidative stress[20]. AuNPs capped by thymidine 5-monophosphate are able to penetrate even into U87 cancer cells nucleus, whereas, those capped with thymine or thymidine only overcome intracellular barriers[21].

Based on these findings, surface modifications of AuNPs have been considered to be crucial for controlling cell uptake, intracellular localization, reduce the cytotoxicity and enhance the biocompatible. The surface functional groups are the base of modifications structures. However, the surface-functional-groups-regulated AuNPs-cells interactions are still poorly understood. The lack of molecular-level details on AuNPs-cell interactions prevents us from gaining an in-depth understanding of the observed phenomena. The goal of this work is to study the surface-functional-groups-regulated AuNPs-cells interaction. We investigated the effect of AuNPs, Au-CH_3 NPs, Au-COOH NPs and Au-OH NPs on human cervical carcinoma (HeLa) cell line and human stomach adenocarcinoma (MCG-803) cell line in vitro. The cell viability and cell cycle has been evaluated when cells are exposed to AuNPs. Moreover, mechanisms of AuNPs-cells interactions have been revealed with micro-Raman spectroscopy.

1 Experimental

1.1 Materials

Chemicals of 11-mercapto-1-undecanol (AR), 11-mercaptoundecanoic acid (AR), 1-undecanethiol and 3-(4, 5-dimethylthiazol-2-yl)-2, 5-diphynyl tetrazolium bromide (MTT, AR) were purchased from Sigma-Aldrich. Chloroaunic acid tetrahydrate ($HAuCl_4 \cdot 4H_2O$) (AR) was obtained from Chengdu Gracia Chemical Technology Company. Sodium citrate ($C_6H_5Na_3O_7$) (AR) was bought from Guangzhou Chemical Regent Factory. All reagents were used without further

purification. Ultrapure water (resistivity ~18.2 MΩ) was used as the solvent throughout the experiments.

1.2 Synthesis, surface modification and characterization of gold nanoparticles

The gold nanoparticles (AuNPs) were synthesized with citrate-mediated reductions[3]. Typically, a stirred aqueous solution of $HAuCl_4$ (0.01%, 50 mL) was heated to reflux, and then trisodium citrate solution (1%, 1.5 mL) was added quickly, resulting in a change in solution color from pale yellow to pink. After the color change, the solution was heated under reflux for an additional 30 min and allowed to cool to room temperature. This procedure resulted in a red solution containing citrate-stabilized AuNPs, and the gold solution was dialyzed for 24 h in deionized water using dialysis membrane (molecular weight cut off 12 kDa) to remove excess unreduced ions in this colloidal solution.

The obtained AuNPs was modified with the most commonly used approach of thiol functionalization[22-23]. Typically, 10 mL of the dialyzed AuNPs solution in a tube was centrifuged at 4000 $r \cdot min^{-1}$ for ~30 min, and the rest of the centrifuged AuNPs with final volume < 50 μL were added to freshly prepared 10 mL of 1 $mmol \cdot L^{-1}$ ethanolic thiol solutions of 11-mercapto-1-undecanol, 11-mercaptoundecanoic acid, 1-undecanethiol, and aged at room temperature for 12 h, respectively. The added alkanethiols amount was estimated to be about 270 molar equivalents to monolayer formation on AuNPs surface at optimum condition. Then, 20 mL of 3 $mol \cdot L^{-1}$ NaCl solution was slowly added into this mixture, followed with sonication for 10 s. This process was repeated 5 times at a 1 h interval to maximize the surface functional groups loading amounts. The functionalized AuNPs were centrifuged three times to remove displaced citrates and excess thiols in solution. The AuNPs solutions were dispersed to achieve a final Au concentration of 39.4 $\mu g \cdot mL^{-1}$. The particle concentration of AuNPs solutions was estimated according to Beers law, with extinction coefficient at 520 nm of 2.78×10^8 $mol^{-1} \cdot cm^{-1}$ [24]. The absorption spectra of AuNPs were recorded on a Cary-100 UV (Varian, USA) spectrometer. The quantities of thiols attached on the surface of AuNPs were further estimated to be 3.9%~4.6% compared to unmodified AuNPs, the decomposition of which at about 200 ℃ was tested by thermogravimetric analysis (TGA, Labsys Evo; Setaram, France) in nitrogen gas at a temperature ramp of 10 $℃ \cdot min^{-1}$. Transmission electron microscopy (TEM) images of AuNPs were observed on an H-8100 transmission electron microscope (Hitachi, Japan). The AuNPs with and without surface modification were dispersed in deionized water to achieve the same Au concentration of 197 $ng \cdot mL^{-1}$. Furthermore, ζ potentials of these AuNPs solutions were measured with electrophoretic light scattering method using a Nano-ZS90 Zeta potentiometry (Malvern, UK) at room temperature.

1.3 Gold nanoparticles treatment and cytotoxicity determination by MTT assay

HeLa cell line and MGC-803 cell line were cultured with dulbeccos modified eagles medium (DMEM) contained 10% fetal calf serum, streptomycin ($1 mg \cdot mL^{-1}$) and penicillin ($1\ 000$ units $\cdot mL^{-1}$), at 37 ℃ in water-saturated air supplemented with 5% CO_2 in CO281R CO_2 cell culture apparatus (New Brunswick Scientific, USA). Actively growing HeLa cells and MGC-803 cells were seeded at a density of 1×10^5 cells $\cdot well^{-1}$ of a 96-well tissue culture plate and incubated overnight. The cells were treated with AuNPs, Au-CH_3 NPs, Au-COOH NPs and Au-OH NPs for 24 and 48 h in quadruplets at a serial of concentrations (c_{Au}: 19.7, 49.25, 98.5 and 197 $ng \cdot mL^{-1}$), respectively. Control cells were used without AuNPs treatment. At the end of each exposure, the cytotoxicity level of AuNPs was assessed by MTT assay measured at 570 nm using an Infinite M1000 UV-Vis microplate reader (TECAN, Austria). All experiments were performed 3 times, and the average of all experiments has been shown as cell-viability percentage in comparison with the control experiment, while AuNPs untreated controls were considered as 100% viable.

1.4 Flow cytometric analysis of cell-cycle

HeLa cells cultured and treated with AuNPs, Au-

CH_3 NPs, Au-COOH NPs and Au-OH NPs at Au concentrations of 197 ng·mL^{-1} for 48 h. In brief, 1×10^5 cells were collected and washed in PBS, slowly fixed in 75% ethanol, and kept at −20 ℃ for 1 h. The cell pellet was centrifuged for 5 min at 2 500 r·min^{-1} and the pellet re-suspended in 0.5 mL RNase (Sigma, 100 μg·mL^{-1}) and stored at 37 ℃ about 30 min. Then, propidium iodide (PI, Sigma, 0.05 mg·mL^{-1}) was added into the cell pellet and incubated for 30 min at 4 ℃. Total cellular DNA content was analyzed with a FC500 flow cytometer (Beckman Coulter Inc., Brea, CA, USA).

1.5 Raman microspectrometry of single living cells treated with AuNPs nanoparticles

HeLa cells were cultured as above and incubated with AuNPs and surface modified AuNPs at Au concentration of 197 ng·mL^{-1} for 48 h. The living cells were analyzed as monolayers, seeding on the cover glass and washed 3 times with PBS. The Raman spectra of single living cells were recorded on the cover glass by confocal Raman spectrometer (Renishaw, inVia, UK) connected to a Leica microscope with a 514-nm emitting. An excitation beam of ~20 mW laser power was focused onto a single cell with a 100× objective, and each Raman spectrum was recorded in the range of 500~1 800 cm^{-1} with integration time of 240 s. All obtained spectra were background corrected and normalized to the 1 450 cm^{-1} band.

1.6 Statistical analysis

For statistical analyses, each experimental value was compared to its corresponding control. Results were expressed as mean ± standard deviation (S.D.). Multi-group comparisons of means were carried out using Student t test. Statistical significance for all tests was set at $p<0.05$.

2 Results and discussion

2.1 Physicoc hemical characterization of surface modified of gold nanoparticles

The citrate-synthesized AuNPs are ones with surface modified by thiols functionalization in aqueous solution. In this most commonly used approach [22-23], three alkanethiols agents with terminal functional groups of -CH_3, -COOH and -OH are adsorbed at the surface of AuNPs via citrate-to-thiol exchanges, generating functionalized Au-CH_3 NPs, Au-COOH NPs and Au-OH NPs, separately (Fig.1). The ligand exchange of thiols for citrate molecules on AuNPs is made due to the substantial difference in energy between Au-S (~168 kJ·mol^{-1})[25] and Au-O (~8 kJ·

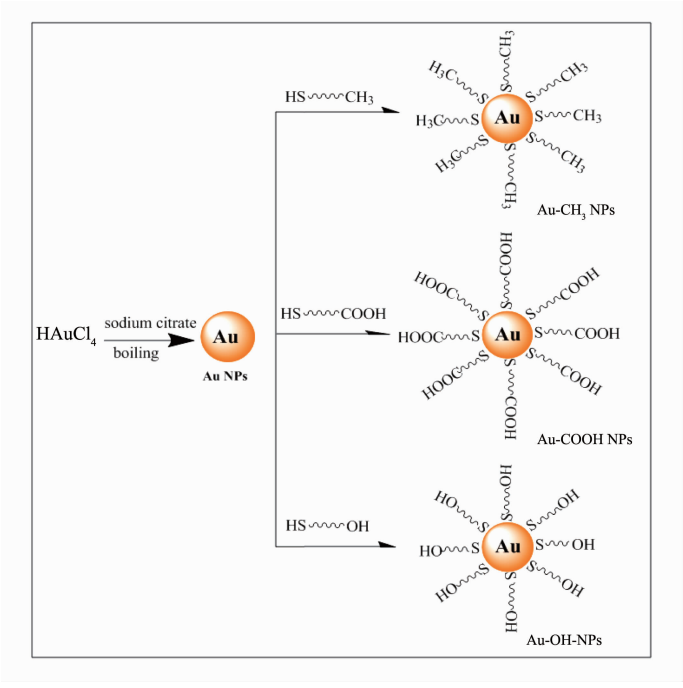

Fig.1 Schematic illustration of the surface modified gold nanoparticles

mol^{-1}) interactions[26]. The self-assembled monolayers with functional groups are formed on surface of AuNPs due to the strong affinity, and structural characterizations of functional groups in overlayer have been probed by attenuated total reflection-infrared intensity (ATR-IR) features and X-ray photoelectron spectroscopy (XPS) data in previous studies[22-23]. Quantitative determination results show that these thiols attached on the surface of AuNPs under optimum condition are approximate, estimated to be 3.9%~4.6%, which is slightly larger than that reported values in literature[22], attributed the smaller size of AuNPs.

The as-prepared AuNPs are observed under transmission electron microscopy (TEM), showing unmodified AuNPs and surface modified AuNPs are roughly spherical, and the average diameters are all about (15.6±3.2) nm (Fig.2). For further characterization, dynamic light scattering (DLS) results show that corresponding average hydrodynamic diameters of the AuNPs, Au-CH_3 NPs, Au-COOH NPs and Au-OH NPs are (21.59±7.98), (30.68±9.24), (25.84±9.84) and (25.0±10.71) nm, respectively. The difference in the average diameters by the two techniques of DLS and TEM is expected considering that TEM measures the size of the electron-dense Au core, whereas DLS measures the capping agent shell and the hydration sphere of the AuNPs [27]. After functionalized with alkanethiols, there are small increases in the hydrohynamic diameter, probably due to the different surface properties imparted by the capping agents. AuNPs are known to exhibit a surface plasmon resonance (SPR) in the visible region, which is caused by incoming electromagnetic radiation indu-cing the formation of a dipole in the nanoparticle[24]. As the UV-Vis spectra shown in Fig.3, the well-defined and narrow SPR absorption of the AuNPs solution is localized at 519 nm, which shifts slightly to 521 nm with an insignificant broadening for Au-CH_3 NPs, Au-COOH NPs and Au-OH NPs solutions. The observation about SPR bands in absorption spectra (Fig.3) indicates that the surface modification does not bring obvious aggregation and difference of particle sizes is very small, which is also proved by TEM (Fig. 2) and DLS results. Both the prepared AuNPs and surface modified AuNPs are wine-red colloidal solution (inset, Fig.2) with the stability over 4 weeks.

For further characterization, ζ potential measurements are carried out to identify the surface charge. ζ potential analysis gives potential values of −30.5,

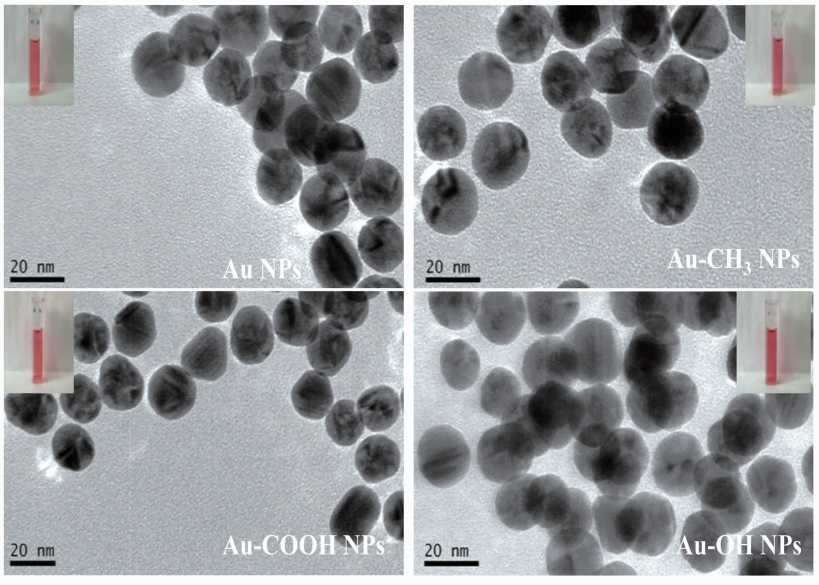

Inset shows the corresponding photographs of as-prepared colloids

Fig.2　TEM images of AuNPs and surface modified AuNPs

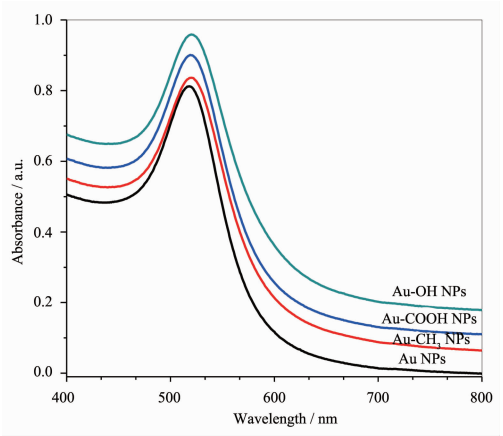

Fig.3 UV-Vis spectra of AuNPs and surface modified AuNPs

−5.43, −44.2 and −34.1 mV for the AuNPs, Au-CH_3 NPs, Au-COOH NPs and Au-OH NPs, respectively. The results reveal that surface of these AuNPs with negative charge. The negative charged spherical AuNPs and surface modified AuNPs with relatively uniform size and stable in the aqueous phase are further used for the interactions studies with cells.

2.2 Cell viability assay and cell-cycle analysis

The biocompatibility of AuNPs, Au-CH_3 NPs, Au-COOH NPs and Au-OH NPs is assessed by MTT assay in vitro. In this work, after treated with AuNPs and surface modified AuNPs at varied Au concentrations from 19.7 to 197 ng·mL^{-1} *in vitro*, cell death is only observed at the highest concentration of 197 ng·mL^{-1} with both HeLa and MCG-803 cells (Fig. 4). The results indicate that the concentration of 197 ng·mL^{-1} is a critical point for cell viability. Consequently, the following studies on AuNPs-cells interaction are investigated at Au concentration of 197 ng·mL^{-1}.

As shown in Fig.4, AuNPs exhibit low cytotoxicity at the highest tested Au concentration of 197 ng·mL^{-1}. The viability of HeLa and MCG-803 cells revealed by MTT data is 79.87% ±3.71% and 76.84% ±3.55% at exposure time of 24 h, which decreases to 72.65% ±2.79% and 71.62% ±2.33% at exposure time of 48 h, respectively. Therefore, an increase in exposure time decreases the percentage of cell viable in the two cell lines, and the cell viability is still higher than 70% . In contrast, higher biocompatibility is detected with these cells following exposure to surface modified AuNPs at the two exposure time point. The viability of HeLa cells is increased to 93.61% ±4.04%, and that of MCG-803 cells is increased to 91.96% ±2.83% after 48 h exposure to Au-OH NPs (Fig.4). This suggests that the modification of functional groups onto the surface of AuNPs is able to render them with improved cytocompatibility in both HeLa and MCG-803 cell lines, and the slight cytotoxicity follows the order AuNPs >Au-CH_3 NPs >Au-COOH NPs ≈Au-OH NPs (Fig.4).

To further explore the bio-effects of AuNPs, Au-CH_3 NPs, Au-COOH NPs and Au-OH NPs, their exposure induced cell-cycle distribution are analyzed with HeLa cells. It is particularly notable that AuNPs exposure leads to an alteration in cell cycle. A

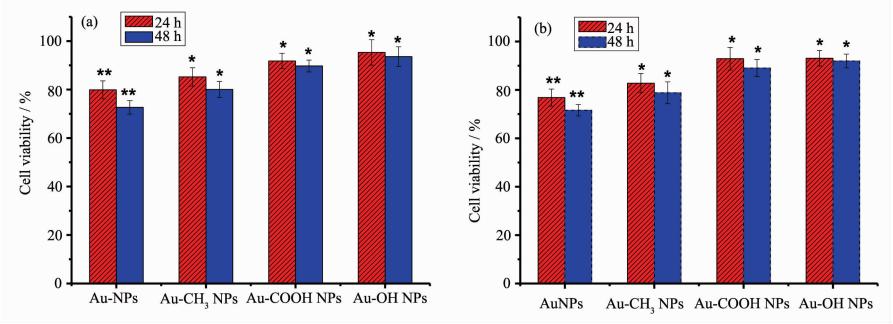

The concentrations of Au are 197 ng·mL^{-1}; All the data were expressed in mean±SD of three independent experiments; *P<0.05, **P<0.01, control versus untreated cells

Fig.4 MTT viability assay of (a) HeLa cells and (b) MCG-803 cells exposed to the AuNPs and surface modified AuNPs, respectively

decrease in G0/G1 phase and an obvious increase in G2/M are noticed after 48 h treatment with AuNPs (Fig.5).The G2/M proportion is 7.74% in control, which increases to 19.43% following exposure to the AuNPs, indicating the AuNPs induce a significant delay of G2/M phase in connection with genotoxicity [28]. In contrast, as shown in Fig.5B ~D, HeLa cell treatment with surface modified AuNPs at the same dosage, the G2/M proportions increase to 14.05% (Au-CH_3 NPs), 13.58% (Au-COOH NPs) and 13.48% (Au-OH NPs), indicating that the surface modified AuNPs evidently decrease the G2/M phase delay effect of AuNPs. The smaller changes of G2/M arrest induced by Au-CH_3 NPs, Au-COOH NPs and Au-OH NPs mean higher cytocompatibility and lower genotoxicity surface modified AuNPs, which is consistent with the above MTT assay results.

2.3 Surface-functional-groups-regulated AuNPs-cells interaction

Micro-Raman spectroscopy is used to obtain rich biochemical information from individual living cells in a non-invasive way, without the need of labels or other contrast [29-33]. As the surface-enhanced Raman spectroscopy (SERS)-active nanoprobe, the endocytic AuNPs are crucial to obtained SERS spectra originated from bio-molecules that are in close proximity to the enhanced electromagnetic field at the Au surface in situ. The Raman spectra of normal HeLa cells and those treated with unmodified and modified AuNPs recorded in the 600 ~1 800 cm^{-1} regions are compared in Fig. 6, and proposed band assignments[30-34] are also included.

Firstly, the influence to phospholipid membrane of the single living HeLa cells is presented in Fig.6. As shown in Fig.6a, the Raman band at 722 cm^{-1} is assigned to the symmetric C-N stretching vibration of phosphatidyl choline headgroup $N^+(CH_3)_3$ [30], which shifts to 726 cm^{-1} and 725 cm^{-1} after treated with AuNPs and Au-CH_3 NPs, respectively (Fig.6b and c). Whereas, these symmetric stretching vibrations are observed at 721 cm^{-1} with slight shifts when treated with Au-COOH and Au-OH NPs (Fig.6d and e). Besides, the intensities of 958 cm^{-1} asymmetric stretching vibration [31] distinctively decrease after treated with AuNPs and Au-CH_3 NPs, while insignificant changes are found with the corresponding peaks with Au-COOH and Au-OH NPs (Fig.6d and e). The peaks at 1 067 and 1 125 cm^{-1} are assigned vibrations of C-C chain stretching of the phospholipid membrane (Fig.6a)[32]. These Raman peaks move to 1

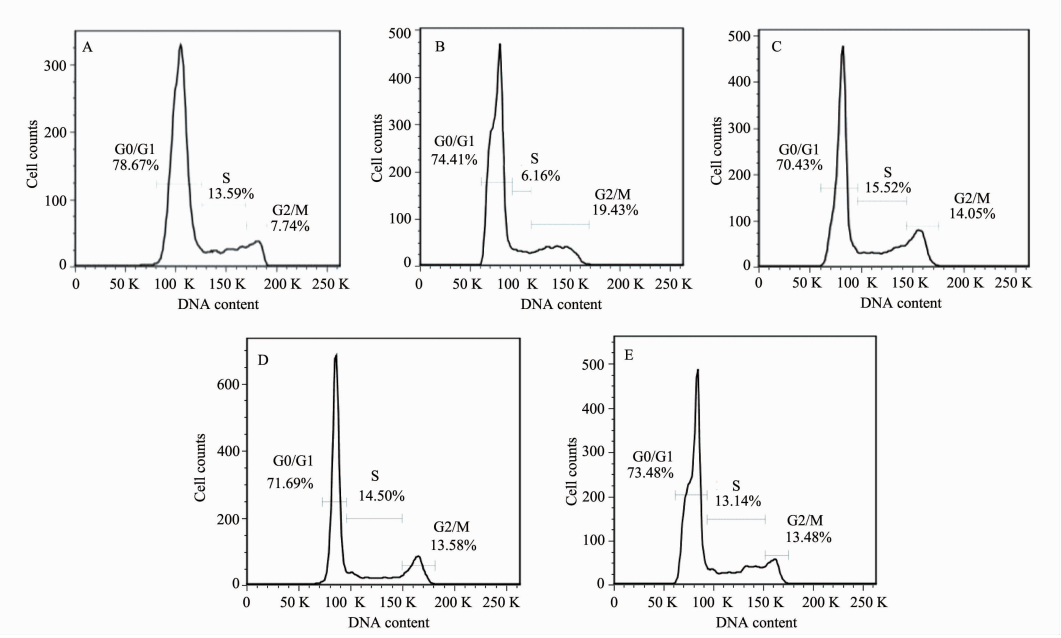

Fig.5　Cell cycle distribution in HeLa cells: (A) HeLa Cells control; HeLa cells exposed to (B) AuNPs; (C) Au-CH_3 NPs; (D) Au-COOH NPs; (E) Au-OH NPs. The concentrations of Au are 197 ng·mL^{-1}

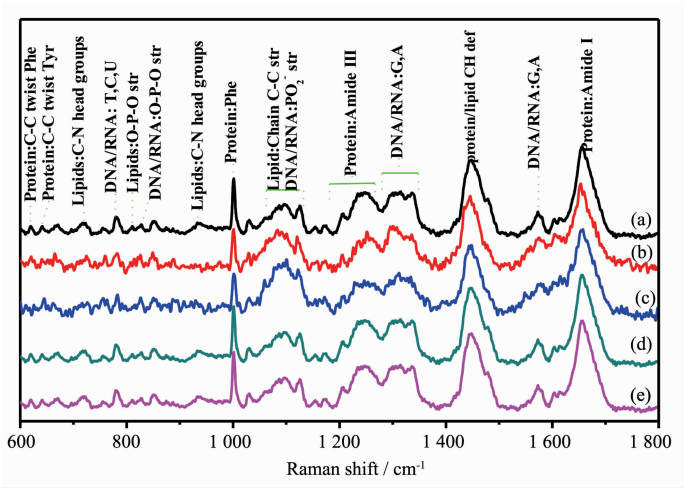

Fig.6 Raman spectra of single living HeLa cells. (a) HeLa cell control; HeLa cell treated with: (b) AuNPs; (c) Au-CH_3 NPs; (d) Au-COOH NPs; (e) Au-OH NPs. The concentrations of Au are 197 ng·mL^{-1}

071 cm^{-1}, 1 126 cm^{-1} induced by AuNPs (Fig.6b), and are observed at 1 068 cm^{-1}, 1 120 cm^{-1} induced by Au-CH_3 NPs (Fig.6c). The corresponding Raman peaks are shown at 1 068 cm^{-1}, 1 123 cm^{-1} for Au-COOH NPs (Fig.6d), and no shifts induced by Au-OH NPs are observed (Fig.6e). Furthermore, the intense mode at 1 449 cm^{-1} assigned to protein and lipid CH deflexed bending mode (Fig.6a)[32] moves to 1 444 cm^{-1} due to treatment of the AuNPs, however, the bands remain approximately constant (Fig.6b ~e) with the surface modified Au NPs. The data suggest that polar choline headgroups of phospholipid membrane are target sites for AuNPs and Au-CH_3 NPs in cells. Besides, the binding of AuNPs and Au-CH_3 NPs disarrange slightly of C-C chains of phospholipid membrane. In contrast, the special interactions on phospholipid membrane are obviously decreased induced by Au-COOH NPs and Au-OH NPs.

Secondly, Raman spectral profiles provide information about DNA-AuNPs interactions in HeLa cells. Especially, the band assigned to the phosphate diester (PO_2^-) symmetric stretching mode of the DNA backbone shifts from 1 097 cm^{-1} (Fig.6a) to 1 102 and 1 100 cm^{-1} after interaction with AuNPs and Au-CH_3 NPs (Fig.6b and c), respectively. The most significant spectral changes are also observed at 827 cm^{-1} peaks (Fig.6a) corresponding to the phosphodiester (O-P-O) stretching bond of DNA backbone[33-34], which move to 824 cm^{-1} after treatment with AuNPs or Au-CH_3 NPs (Fig.6b and c). Whereas, the treatments with Au-COOH NPs and Au-OH NPs have no significant contribution for both O-P-O and PO_2^- stretching vibrations in the spectra (Fig.6d and e). Besides, the vibrational mode observed at 782 cm^{-1} correlates with cytosine ring breathings of pyrimidine, and 1 337 cm^{-1} assigned to adenine (A) and guanine (G) ring stretching[33-34] shift to 778 and 1 331 cm^{-1} induced by Au NPs, respectively (Fig.6b). These Raman bands show insignificant changes as treated with Au-CH_3 NPs, Au-COOH NPs and Au-OH NPs (Fig.6c ~e). According to this observation, the basic assumption is that the backbone and nucleic bases of DNA molecules have chemisorptions occurring on the surface of AuNPs. Whereas, AuNPs modified with -COOH and -OH can obviously decrease this surface interaction.

Interestingly, exposure to AuNPs induces obvious spectral changes with Raman peaks associated with the polar headgroup of phospholipid membrane, and Raman vibrations are attributed to backbone and nucleic bases of DNA. Therefore, our micro-Raman results provide the evidence *in situ* that the polar headgroup of phospholipid membrane and backbone and nucleic bases of DNA are probably the targeted sites of AuNPs-cells interaction. The detected difference suggests that AuNPs and surface modified

AuNPs exposure displays different effect on DNA and phospholipid membrane, following the order AuNPs > Au-CH_3 NPs >Au-COOH NPs ≈Au-OH NPs. The conclusion also supports the cytotoxicity results of Au-CH_3 NPs attained by MTT assay, and is consistent with the flow cytometry results of cell cycle G2/M arrest. The present studies determine the difference interactions of AuNPs containing a variety of surface functional groups with cells. The surface-functional-groups-regulated interactions provide the probable mechanism to explain the surface-modified regulated cytotoxicity of AuNPs, although further experiments would be necessary to conclusively demonstrate this.

3 Conclusions

Taken together, negative charged spherical and stable AuNPs, Au-CH_3 NPs, Au-COOH NPs and Au-OH NPs with diameter ~16 nm have been prepared. The data suggest that the surface unmodified AuNPs exhibit low cytotoxicity at the highest concentration of 197 ng·mL^{-1} for both HeLa and MCG-803 cells *in vitro*, and induce a cell cycle slightly arrest in the G_2/M phase. The surface modified AuNPs can further decrease the inherently cytotoxicity that follows the order AuNPs>Au-CH_3 NPs>Au-COOH NPs ≈Au-OH NPs. Our results demonstrate the molecular mechanism *in situ* that the polar headgroup of phospholipid membrane, backbone and nucleic bases of DNA are the mainly interacted target sites of the AuNPs and Au-CH_3 NPs in living cells. In contrast, the binding to these sites are insignificant induced by Au-COOH NPs and Au-OH NPs.

Acknowledgements: The Authors are grateful to Professor SHEN Pan-Wen at Nankai University for providing us long-term support, attention and guidance.

References:

[1] Yeh Y C, Creran B, Rotello V M. *Nanoscale*, **2012**,**4**:1871-1880

[2] Daniel M C, Astruc D. *Chem. Rev*., **2004**,**104**:293-346

[3] Turkevich J, Stevenson P C, Hillier J. *Discuss. Faraday Soc*., **1951**,**11**:55-75

[4] Frens G. *Nat. Phys. Sci*., **1973**,**241**:20-22

[5] Giljohann D A, Seferos, D S, Daniel W L, et al. *Angew. Chem. Int. Ed*., **2010**,**49**:3280-3294

[6] Wang Z, Tan B, Hussain I, et al. *Langmuir*, **2007**,**23**:885-895

[7] Ding Y, Bian X, Yao W, et al. *ACS Appl. Mater. Inter*., **2010**,**2**:1456-1465

[8] Huang P, Bao L, Zhang C, et al. *Biomaterials*, **2011**,**32**:9796-9809

[9] Wu P, Hwang K, Lan T, et al. *J. Am. Chem. Soc*., **2013**,**135**:5254-5257

[10]Bartczak D, Nitti S, Millar T M, et al. *Nanoscale*, **2012**,**4**:4470-4472

[11]Park J, Park J H, Ock K S, et al. *J. Colloid Interface Sci*., **2011**,**363**:105-113

[12]Ghosh R, Singh L C, Shohet J M, et al. *Biomaterials*, **2013**,**34**:807-816

[13]Wang F, Wang Y-C, Dou S, et al. *ACS Nano*, **2011**,**5**:3679-3692

[14]Heo D N, Yang D H, Kwon K. *Biomaterials*, **2012**,**33**:856-866

[15]Mieszawska A J, Mulder W J M, Fayad Z A, et al. *Mol. Pharmaceutics*, **2013**,**10**:831-847

[16]Jans H, Huo Q. *Chem. Soc. Rev*., **2012**,**41**:2849-2866

[17]Pan Y, Neuss S, Leifert A, et al. *Small*, **2007**,**3**:1941-1949

[18]Goodman C M, McCusker C D, Yilmaz T, et al. *Bioconjugate Chem*., **2004**,**15**:897-900

[19]Connor E E, Mwamuka J, Gole A, et al. *Small*, **2005**,**1**:325-327

[20]Pan Y, Leifert A, Ruau D, et al. *Small*, **2009**,**5**:2067-2076

[21]Avvakumova S, Scari G, Porta F. *RSC Adv*., **2012**,**2**:3658-3661

[22]Park J-W, Shumaker-Parry J S. *ACS Nano*, **2015**,**9**:1665-1682

[23]Zhou Y, Wang S X, Zhang K, et al. *Angew. Chem*., **2008**, **120**:7564-7566

[24]Zhao W, Chiuman W, Lam J C F, et al. *J. Am. Chem. Soc*., **2008**,**130**:3610-3618

[25]Nuzzo R G, Zegarski B R, Dubois L H. *J. Am. Chem. Soc*., **1987**,**109**:733-740

[26]Chen F, Li X, Hihath J, et al. *J. Am. Chem. Soc*., **2006**,**128**:15874-15881

[27]Jiang B P, Zhang L, Zhu Y, et al. *J. Mater. Chem. B*, **2015**,**3**:3767-3776

[28]Jeyaraj M, Arun R, Sathishkumar G, et al. *Mater. Res. Bull*., **2014**,**52**:15-24

[29]Puppels G J, de Mul F F, Otto C, et al. *Nature*, **1990**,**347**:301-303

[30]Konorov S O, Schulze H G, Piret J M, et al. *J. Raman Spectrosc*., **2011**,**42**:1135-1141

[31]Bush S F, Adams R G, Levin I W. *Biochemistry*, **1980**,**19**: 4429-4436

[32]Notingher I, Verrier S, Haque S, et al. *Biopolymer*, **2003**,**72**: 230-240

[33]Zoladek A, Pascut F C, Patel P, et al. *J. Raman Spectrosc*., **2011**,**42**:251-258

[34]Pyrgiotakis G, Kundakcioglu O E, Pardalos P M, et al. *J. Raman Spectrosc*., **2011**,**42**:1222-1231